

The Vienna LTE Simulators - Enabling Reproducibility in Wireless Communications Research

Christian Mehlführer, Josep Colom Ikuno, Michal Šimko, Stefan Schwarz, Martin Wrulich, and Markus Rupp

Abstract—In this paper, we introduce MATLAB-based link and system level simulation environments for UMTS Long Term Evolution (LTE). The source codes of both simulators are available under an academic non-commercial use license allowing researchers full access to standard-compliant simulation environments. Due to the open source availability, the simulators enable reproducible research in wireless communications and comparison of novel algorithms.

In this work, we explain how link and system level simulations are connected and show how the link level simulator serves as a reference to design the system level simulator. We compare the accuracy of the PHY modeling at system level by means of simulations performed both with bit-accurate link level simulations and PHY-model-based system level simulations. We point out some of the currently most interesting research questions for LTE, and explain by some research examples how our simulators can be applied.

Index Terms—LTE, MIMO, link level, system level, simulation, reproducible research

I. INTRODUCTION

Reproducibility is one of the pillars of scientific research. Whereas reproducibility has a long tradition in most nature sciences and theoretical sciences, such as mathematics, it is only recently that reproducible research becomes more and more important in the field of signal processing [2, 3]. In contrast to results in fields of purely theoretical sciences, results of signal processing research papers can only be reproduced if a comprehensive description of the investigated algorithms (including the setting of all necessary parameters), as well as eventually required input data are fully available. Due to lack of space, a fully comprehensive description of the algorithm is often omitted in research papers. Even if an algorithm is explained in detail, for instance by a pseudo code, initialization values are often not fully defined. Moreover, it is often not possible to include in a paper all necessary resources, such as data, that was processed by the presented algorithms. Ideally, all resources, including source code of the presented algorithms, should be made available for download to enable other researchers (and also reviewers of papers) to reproduce the results presented. **Unfortunately, researcher’s reality does not resemble this ideal situation, a circumstance that has recently been complained about quite openly [4].**

C. Mehlführer, J. Colom Ikuno, M. Šimko, S. Schwarz, and M. Rupp are with the Institute of Telecommunications, Vienna University of Technology, Austria; email: {chmehl, jcolom, msimko, sschwarz, mrupp}@nt.tuwien.ac.at
M. Wrulich is with McKinsey&Company, Hamburg, Germany; email: mwruulich@gmail.com

In the past years, several researchers have started to build up online resource databases in which simulation code and data is provided, see for example [5, 6]. However, it is still not a common practice in signal processing research. We are furthermore convinced that reproducibility should also play an important role in the review process of a paper. Although thorough checking is very possibly impractical, it would make the presented works more transparent to the review process. Reproducibility becomes even more important when the systems that are simulated become more and more complex, as it is the case in the evaluation of wireless communication systems. When algorithms for wireless systems are evaluated, authors often claim to use a standard-compliant transmission system and simply reference to the corresponding technical specification. Since technical specifications are usually extensive, including a cornucopia of options, it is not always clear which parts of a specification were actually implemented and which parts were omitted for simplicity reasons. **The situation of trying to reproduce someone else’s results in order to compare them to your own algorithm but not being able to do so (or only after extensive effort to discover the unreported details of the actual implementation) is familiar to most researchers. Without access to the details of the implementation including all assumptions, comparisons of algorithms, developed by different researchers, are very difficult, if not impossible to carry out.** A way out of this dilemma is offered by a publicly available simulation environment. In this work, we present such an open-source simulation environment that allows to carry out link and system level simulations of the Universal Mobile Telecommunications System (UMTS) Long Term Evolution (LTE), specifically designed to support reproducibility. The development and publishing of this LTE simulation environment is based on our previous, very good experience with a WiMAX physical layer simulator [7].

Furthermore, such simulators can be used as a reference for validation of algorithms, for example when designing transmitter or receiver chips [8]. We also have used our simulators for generating LTE signals that are required to include realistic signals in related research [9], or as a reference for LTE-compliant measurements. Here, the simulator can serve not only as a data pump but also as a vehicle to evaluate the received data.

LTE is the current evolutionary step in the third Generation Partnership Project (3GPP) roadmap for future wireless cellular systems. LTE was introduced in 3GPP Release 8 [10],

which—besides the definition of the novel physical layer—also contains many other remarkable innovations. Most notable are (i) the redevelopment of the system architecture, now called System Architecture Evolution (SAE), (ii) the definition of network self-organization, and (iii) the introduction of home base-stations. The main reasons for these profound changes in the Radio Access Network (RAN) system design are to provide higher spectral efficiency, lower delay (latency), and more multi-user flexibility than the currently deployed networks.

In the development and standardization of LTE, as well as in the implementation process of equipment manufacturers, simulations are necessary to test and optimize algorithms and procedures. This has to be carried out on the physical layer (link level) and in the network (system level) context:

- 1) *Link level simulations* allow for the investigation of channel estimation, tracking, and prediction algorithms, synchronization algorithms [13, 14], Multiple-Input Multiple-Output (MIMO) gains, Adaptive Modulation and Coding (AMC) and feedback [15, 16]. Furthermore, receiver structures (typically neglecting inter-cell interference and impact of scheduling, as this increases simulation complexity and runtime dramatically) [17], modeling of channel encoding and decoding [18], physical-layer modeling crucial for system level simulations [19] and alike are typically analyzed on link level. Although MIMO broadcast channels have been investigated quite extensively over the last years [20, 21], there are still a lot of open questions that need to be resolved, both in theory and in practical implementation. For example, LTE offers the flexibility to adjust many transmission parameters, but it is not clear up to now how to exploit the available Degrees of Freedom (DoF) to achieve the optimum performance. Some recent theoretical results point out how to proceed in this matter [21, 22], but practical results for LTE are still missing.
- 2) *System level simulations* focus more on network-related issues, such as resource allocation and scheduling [23, 24], multi-user handling, mobility management, admission control [25], interference management [26, 27], and network planning optimization [28, 29]. On top of that, in a multi-user oriented system, such as LTE, it is not directly clear which figures of merit should be used to assess the performance of the system. The classical measures of (un)coded Bit Error Ratio (BER), (un)coded BLock Error Ratio (BLER), and throughput are not covering multi-user scenario properties. More comprehensive measures of the LTE performance are for example *fairness*, *multi-user diversity*, or *DoF* [30]. However, these theoretical concepts have to be mapped to performance values that can be evaluated by means of simulations [31, 32].

Around the world, many research facilities and vendors are investigating the above mentioned aspects of LTE. For that purpose, commercially available simulators applied in industry [33–35], as well simulators applied in academia [36] have been developed. Also, probably all major equipment

vendors have implemented their own, proprietary simulators. Regardless of the simulation tools being commercial/non-commercial, the development framework (C, C++, MATLAB, WM-SIM [36], ...), or their claimed performance/flexibility, one fact is shared by all of the simulators. **Their closed implementation disables access to implementation details and thus to any assumption that may have been included. As such the reliability of the results relies purely on the faith of a proper implementation. Independent validation of results in such closed simulation environments is not easy, very time-consuming and often not feasible.** People familiar with RAN standardization know how difficult it is to compare and even align simulation results. Since the results were obtained with closed tools, simply repeating the same experiment is a daunting task. Transparency not only in the results but also in the tools employed, thus greatly magnifies the credibility of the results.

The two simulators [37, 38] described in Sections II and III of this paper are freely available at our homepage [1] under an open, free for non-commercial academic use license, which facilitates academic research and enables a closer cooperation between different universities and research facilities. In addition, developed algorithms can be shared under the same license again, making the comparison of algorithms easier, reproducible, and therefore refutable and more credible. To the best of the authors' knowledge, our two simulators are the first to be published in context of LTE including source code under an academic use license. Thus, the simulators provide opportunities for many institutions to directly apply their ideas and algorithms in the context of LTE. **The availability of the simulators together with the possibility to include links to the utilized simulator version and any resources needed furthermore enables researchers to quickly reproduce published results [3].**

The remainder of this paper is organized as follows. In Sections II and III, we describe the *Vienna LTE Simulators* and how they relate to each other. In Section IV we provide a validation of the two simulators. Exemplary simulation results are shown in Section V. Finally, we conclude the paper in Section VI.

II. THE VIENNA LTE LINK LEVEL SIMULATOR

In this section, we describe the overall structure of the Vienna LTE Link Level Simulator, currently (January 2011) released in version 1.6r917. Furthermore, we present the capabilities of the simulator and provide some examples of its application.

A. Structure of the Simulator

The link level simulator can be divided into three basic building blocks, namely *transmitter*, *channel model*, and *receiver* (see Figure 1). Depending on the type of simulation, one or several instances of these basic building blocks are employed. The transmitter and receiver blocks are linked by the channel model, which is used to transmit the downlink data, while signaling and uplink feedback is assumed to be error-free. **Since signaling is stronger protected than**

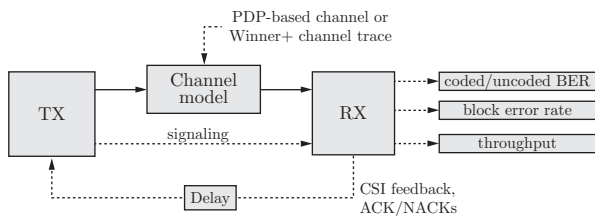


Fig. 1. LTE link level simulator structure, as implemented in the Vienna LTE link level simulator.

data, by means of lower coding rates and/or lower-order modulations, the assumption of error-free signaling is in fact quite realistic. Equivalently, errors on the signaling channels will only occur when the data channels are already using large amounts of performance degradation — a point of operation usually not targeted in investigations.

In the downlink, the signaling information passed on by the transmitter to the receiver contains coding, HARQ, scheduling, and precoding parameters. In the uplink, Channel Quality Indicator (CQI), Precoding Matrix Indicator (PMI), and Rank Indicator (RI) (all three together forming the Channel State Information (CSI)) are signaled. All simulation scenarios (see Section II-B) support the feedback of CQI, PMI, and RI, although it is also possible to set some or all of them to fixed values. Such a setting is required for specific simulations, such as throughput evaluation of a single Modulation and Coding Scheme (MCS).

A standard-compliant implementation of the downlink control channels would not affect the overall structure of our simulator and just requires the insertion of the control channels in the relevant resource elements [39]. On the other hand, non-error-free feedback transmissions would require a physical layer implementation of the LTE uplink, which is currently not in the scope of the simulator.

1) *Transmitter*: The layout of the transmitter is shown in Figure 2. This structure is basically a graphical representation of the transmitter description defined in the TS36' standard series [39–41]. Based on User Equipment (UE) feedback values, a scheduling algorithm assigns Resource Blocks (RBs) to UEs and sets an appropriate MCS (coding rates between 0.076 and 0.926 with 4, 16, or 64-QAM modulation [41]), the MIMO transmission mode (Transmit Diversity (TxD), Open Loop Spatial Multiplexing (OLSM), or Closed Loop Spatial Multiplexing (CLSM)), and the precoding/number of spatial layers for all served users. Such a channel adaptive scheduling allows the exploitation of frequency diversity, time diversity, spatial diversity, and multi-user diversity.

Given the number of available DoF, the specific implementation of the scheduler algorithm has a large impact on the system performance and is a hot topic in research [42–44]. In Section V-B, we provide performance evaluations of several schedulers.

2) *Channel Model*: The Vienna LTE Link Level Simulator supports block and fast fading channels. In the block fading case, the channel is constant during the duration of

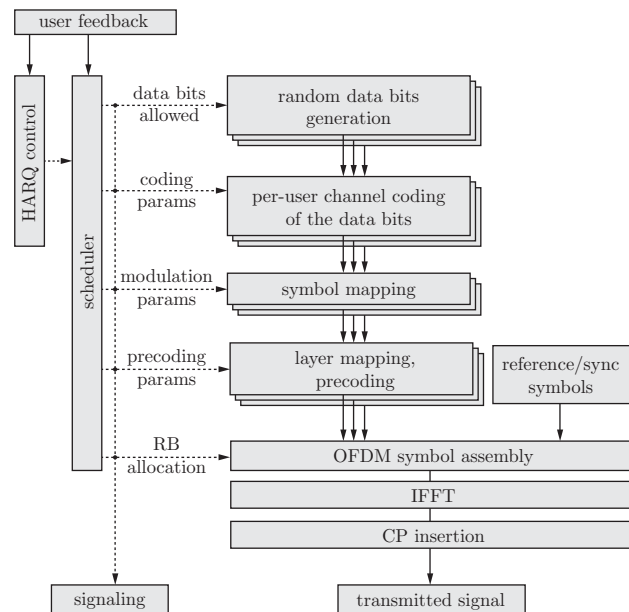


Fig. 2. LTE downlink transmitter structure, as implemented in the Vienna LTE link level simulator.

one subframe (1 ms). In the fast fading case, time-correlated channel impulse responses are generated for each sample of the transmit signal. Currently (January 2011), the simulator supports the following channel models:

- 1) Additive White Gaussian Noise (AWGN)
- 2) Flat Rayleigh fading
- 3) Power Delay Profile-based channel models such as ITU Pedestrian B, or ITU Vehicular A [45]
- 4) Winner Phase II+ [46]

The most sophisticated of these channel models is the Winner Phase II+ model. It is an evolution of the 3GPP spatial channel model and introduces additional features such as support for arbitrary 3D antenna patterns.

3) *Receiver*: Figure 3 shows our implementation of the UE receiver. After disassembling the RBs according to UE resource allocation, MIMO Orthogonal Frequency Division Multiplexing (OFDM) detection is carried out. The simulator currently supports Zero-Forcing (ZF), Linear Minimum Mean Squared Error (LMMSE), and soft sphere decoding as detection algorithms. The detected soft bits are decoded to obtain the data bits and several figures of merit, such as coded/uncoded BER, BLER, and throughput.

Currently, four different types of channel estimators are supported within the simulator: (i) Least Squares (LS), (ii) Minimum Mean Squared Error (MMSE), (iii) Approximate LMMSE [47], and (iv) genie-driven (near) perfect channel knowledge based on all transmitted symbols.

LTE requires UE feedback in order to adapt the transmission to the current channel conditions. The LTE standard specifies three feedback indicators for that purpose, CQI, RI and PMI [39]. The CQI is employed to choose the appropriate MCS, such to achieve a predefined target BLER, whereas the RI and the PMI are utilized for MIMO pre-processing. Specifically, the RI informs the eNodeB about the preferred number of parallel spatial data streams, while the PMI

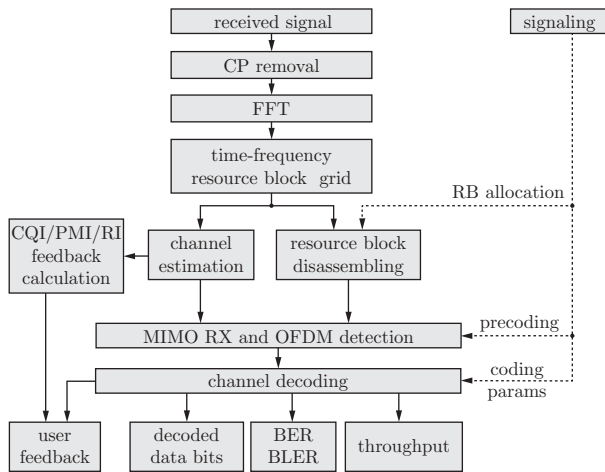


Fig. 3. LTE downlink receiver structure, as implemented in the Vienna LTE link level simulator.

signals the preferred precoder that is stemming from a finite code book as specified in [39]. Very similar feedback values are also employed in other systems such as WiMAX and WiFi. The simulator provides algorithms that utilize the estimated channel coefficients to evaluate these feedback indicators [16]. Researchers and engineers working on feedback algorithms can implement other algorithms by using the provided feedback functions as a starting point to define their own functions.

Given this receiver structure, the simulator allows to investigate various aspects, such as frequency synchronization [48], channel estimation [47], or interference awareness [49].

B. Complexity

Link level simulators are in practice a direct standard-compliant implementation of the Physical (PHY) layer procedures, including segmentation, channel coding, MIMO, transmit signal generation, pilot patterns, and synchronization sequences. Therefore, implementation complexity and simulation time are high. To obtain a simulator with readable and maintainable code, a high level language (MATLAB) has been chosen. This choice enabled us to develop the simulator in a fraction of the time required for an implementation in other languages such as C. Furthermore, MATLAB ensures cross-platform compatibility. While MATLAB is certainly slower than C, by means of code optimization (vectorization) and parallelization by the MATLAB Parallel/Distributed Computing Toolbox, simulation runtime can be greatly reduced. **Severely difficult-to-vectorize and often-called functions are implemented in C and linked to the MATLAB code by means of MEX functions. Such functions include the channel coding/decoding [50], Cyclic Redundancy Check (CRC) computation [51], and soft sphere decoding.**

Furthermore, it is possible to adjust the scale of the simulation to the specific needs. This is achieved by introducing three different simulation types with largely different computational complexity (Figure 4):

1) *Single-downlink*: This simulation type only covers the link between one eNodeB and one UE. Such a set-up allows for the investigation of channel tracking, channel estimation [47], synchronization [14, 52], MIMO gains, AMC and feedback optimization [16], receiver structures [53] (neglecting interference and impact of the scheduling¹), modeling of channel encoding and decoding [18, 54], and physical layer modeling [55], which can be used for system level abstraction of the physical layer. To start a simple single-downlink simulation, run the file `LTE_sim_batch_single_downlink.m`.

2) *Single-cell multi-user*: This simulation covers the links between one eNodeB and multiple UEs. This set-up additionally allows for the investigation of receiver structures that take into account the influence of scheduling, multi-user MIMO resource allocation, and multi-user gains. Furthermore, this set-up allows researchers to investigate practically achievable multi-user rate regions. In the current implementation, the simulator fully evaluates the receivers of all users. However, if receiver structures are being investigated, the computational complexity of the simulation can considerably be reduced by only evaluating the user of interest. **In order to enable a functional scheduler it is sufficient to compute just the feedback parameters for all other users.** To start a simple single-cell multi-user simulation, run the file `LTE_sim_batch_single_cell_multi_user.m`.

3) *Multi-cell multi-user*: This simulation is by far the computationally most demanding scenario and covers the links between multiple eNodeBs and UEs. This set-up allows for the realistic investigation of interference-aware receiver techniques [56], interference management (including cooperative transmissions [57] and interference alignment [58, 59]), and network-based algorithms such as joint resource allocation and scheduling. Furthermore, despite the vast computational efforts needed, such simulations are crucial to verify system level simulations. To start a simple multi-cell multi-user simulation, run the file `LTE_sim_batch_multi_cell_multi_user.m`.

The simulation time, which depends mainly on the desired precision and statistical accuracy of the simulation results, the selected bandwidth, the transmission mode, and the chosen modulation order is for most users a crucial factor. It should be noted that by a smart choice of the simulation settings, the simulation time can be decreased (e.g., when investigating channel estimation performance, the smallest bandwidth can be sufficient).

III. THE VIENNA LTE SYSTEM LEVEL SIMULATOR

In this section, we describe the overall structure of the Vienna LTE System Level Simulator, currently (January 2011) version 1.3r427. We furthermore show how the PHY layer procedures have been abstracted in a low complexity manner.

A. Structure of the Simulator

In system level simulations, the performance of a whole network is analyzed. In LTE, such a network consists of a

¹Note that the scheduler in a multi-user system will change the statistics of the individual user's channel, thus influencing the receiver performance.

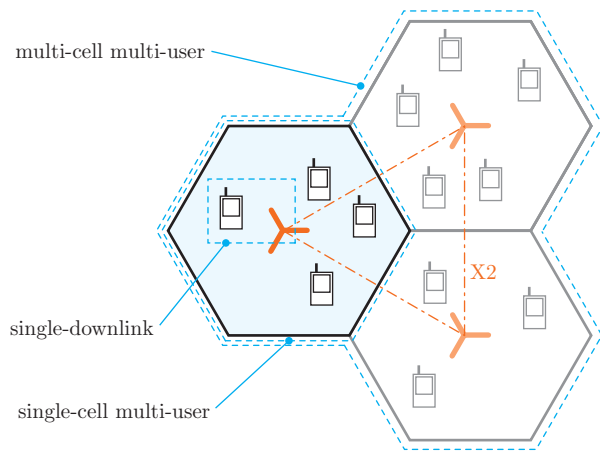


Fig. 4. Three different scenarios in the Vienna LTE link level simulator allow to adjust the scale of the simulation.

376 multitude of eNodeBs that cover a specific area in which many
 377 mobile terminals are located and/or moving around. While
 378 simulations of individual physical layer links allow for the
 379 investigation of MIMO gains, AMC feedback, modeling of
 380 the channel code, and retransmissions [16, 47, 48, 54, 60],
 381 it is not possible to reflect the effects of cell planning,
 382 scheduling, or interference in a large scale with dozens of
 383 eNodeBs and hundreds of users. Simply performing physical
 384 layer simulations of the radio links between all terminals and
 385 base-stations is unfeasible for system level investigations due
 386 to the vast amount of computational power required. Thus,
 387 the physical layer has to be abstracted by simplified models
 388 capturing its essential dynamics with high accuracy at low
 389 complexity.

390 Following the standard approach in literature [55, 61], our
 391 simulator consists of two parts: (i) a link measurement model
 392 and (ii) a link performance model. The link measurement
 393 model reflects the link quality, given by the UE measurement
 394 reports, and is required to carry out link adaptation and
 395 resource allocation. **The chosen link quality measure
 396 is evaluated per subcarrier. Based on the Signal to
 397 Interference and Noise Ratio (SINR), the UE computes
 398 the feedback (PMI, RI, and CQI), which is employed
 399 for link adaptation at the eNodeB as described in Section II-A. The scheduling algorithm assigns resources
 400 to users to optimize the performance of the system
 401 (e.g., in terms of throughput) based on this feed-
 402 back [24]. Following the link measurement model,
 403 the link performance model predicts the BLER of the
 404 link, based on the receiver SINR and the transmission
 405 parameters (e.g., modulation and coding). Figure 5
 406 illustrates the interaction between the two models
 407 and the several physical layer parameters.**

409 Implementation-wise, the simulator follows the structure
 410 shown in Figure 6. Each network element is represented by a
 411 suitable class object, whose interactions are described below.

412 In order to generate the network topology, transmission
 413 sites are generated, to which three eNodeBs are appended,
 414 i.e., sectors, each containing a scheduler (see Figure 6). In
 415 the simulator, traffic modeling assumes full buffers in the

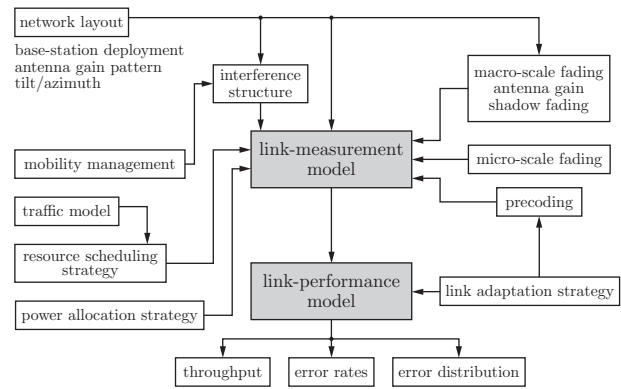


Fig. 5. Schematic block diagram of the LTE system level simulator.

416 downlink. A scheduler assigns PHY resources, precoding
 417 matrices, and a suitable MCS to each UE attached to an
 418 eNodeB. The actual assignment depends on the scheduling
 419 algorithm and the received UE feedback.

420 At the UE side, the received subcarrier post-equalization
 421 symbol SINR is calculated in the link measurement model.
 422 The SINR is determined by the signal, interference, and noise
 423 power levels, which are dependent on the cell layout (defined
 424 by the eNodeB positions, large-scale (macroscopic, macro-
 425 scale) pathloss, shadow fading [62]) and the time-variant
 426 small-scale (microscopic, micro-scale) fading [63].

427 The CQI feedback report is calculated based on the subcar-
 428 rier SINRs and the target transport BLER. The CQI reports are
 429 generated by an SINR-to-CQI mapping [38] and made avail-
 430 able to the eNodeB implementation via a feedback channel
 431 with adjustable delay. **At the transmitter, the appropriate
 432 MCS is selected by the CQI to achieve the target BLER
 433 during the transmission. Especially in high mobility
 434 scenarios, the feedback delay caused by computa-
 435 tion and signaling timing can lead to a performance
 436 degradation if the channel state changes significantly
 437 during the delay.** In the link performance model, an AWGN-
 438 equivalent SINR (γ_{AWGN}) is obtained via Mutual Information
 439 Effective Signal to Interference and Noise Ratio Mapping
 440 (MIESM) [64–66]. In a second step, γ_{AWGN} is mapped to
 441 BLER via AWGN link performance curves [37, 38]. The
 442 BLER value acts as a probability for computing ACK/NACKs,
 443 which are combined with the Transport Block (TB) size
 444 to compute the link throughput. **The simulation output
 445 consists of traces, containing link throughput and
 446 error ratios for each user, as well as a cell aggregates,
 447 from which statistical distributions of throughputs
 448 and errors can be extracted.**

B. Complexity

449 One desirable functionality of a system level simulator is the
 450 ability to precalculate as many of the simulation parameters
 451 as possible. This not only reduces the computational load
 452 while carrying out a simulation, but also offers repeatability
 453 by loading an already partly precalculated scenario.

454 The precalculations involved in the LTE system level sim-
 455 ulator are the generation of (i) eNodeB-dependent large-
 456 scale pathloss maps, (ii) site-dependent shadow fading maps,
 457

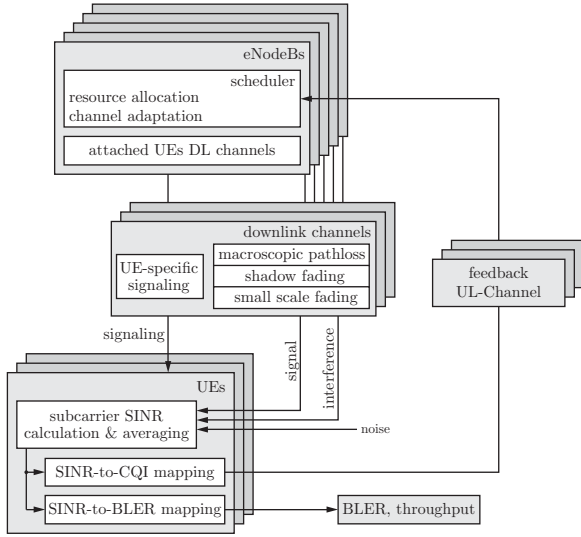


Fig. 6. Schematic class diagram showing the relation between the several components comprising the LTE System Level Simulator.

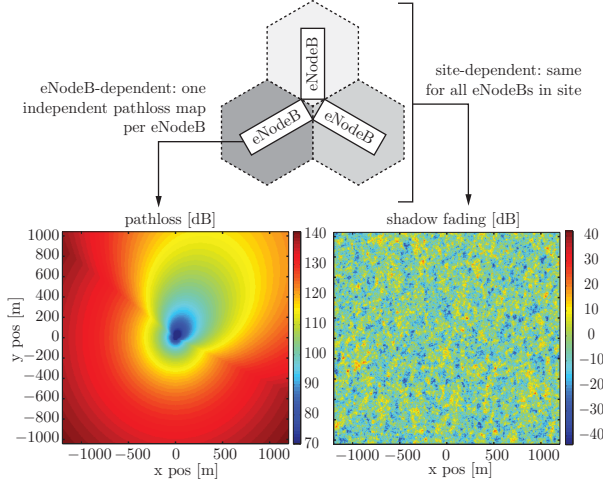


Fig. 7. Left: Large-scale pathloss and antenna gain map [dB] of one eNodeB. Right: space-correlated shadow fading of one site [dB].

and (iii) time-dependent small-scale fading traces for each eNodeB-UE pair.

1) *Pathloss and Fading Maps*: The large-scale pathloss and the shadow fading are modeled as position-dependent maps. The large-scale pathloss is calculated according to well-known models [62, 67] and combined with the antenna gain pattern of the corresponding eNodeB. Space-correlated shadow fading is obtained from a log-normal random distribution using a low-complexity variant of the Cholesky decomposition [68]. Inter-site map correlation for shadow fading is similarly obtained. Figure 7 shows exemplary large-scale pathloss and shadow fading maps.

2) *Time-dependent Fading Trace*: While the large-scale pathloss and the shadow fading are modeled position-dependent, the small-scale fading is modeled as a time-dependent trace. The calculation of this trace is based on the transmitter precoding, the small-scale fading MIMO channel matrix, and the receive filter. Currently, the receiver modeling is based on a linear ZF receiver. The small-scale fading

TABLE I
TEST SCENARIOS OF 3GPP TS 36.101.

	8.2.1.1.1/1	8.2.1.1.1/8	8.2.1.2.1/1	8.2.1.3.2/1
TX mode	single ant.	single ant.	TxD	OLSM
channel	EVEhA	ETU	EVEhA	EVEhA
Doppler freq.	5 Hz	300 Hz	5 Hz	70 Hz
modulation	QPSK	16QAM	16QAM	16QAM
code rate	1/3	1/2	1/2	1/2
$N_T \times N_R$	1×2	1×2	2×2	4×2
antenna corr.	low	high	medium	low
channel SNR req.	-1 dB	9.4 dB	6.8 dB	14.3 dB

trace consists of the signal power and the interference power after the receive filter. The break-down into these two parts significantly reduces the computational effort since it avoids many complex multiplications required when directly working with MIMO channel matrices on system level [19, 38, 55].

IV. VALIDATION OF THE SIMULATORS

Validation of the simulators was performed in two steps. Firstly, in Section IV-A we compared the link level throughput with the minimum performance requirements stated by 3GPP in the technical specification TS 36.101 [69]. Secondly, in Section IV-B we cross-validated the link and the system level simulators by comparing their results against each other. Other means of validation are being discussed in Section IV-C.

A. 3GPP Minimum Performance Requirements

The technical specification TS 36.101 [69] defines minimum performance requirements for a UE that utilizes a dual-antenna receiver. These requirements have to be met by real devices and therefore have to be surpassed by our simulator, **in which not every conceivable influential factor is incorporated.**² Such factors may include frequency and timing synchronization as well as other non-ideal effects, such as quantization or non-ideality of the manufactured physical components (e.g., I/Q imbalances, phase noise, power amplifier nonlinearities).

In particular, TS 36.101 specifies reference measurement channels for the Physical Downlink Shared Channel (PDSCH) (comprising bandwidth, AMC scheme, overhead, ...) and propagation conditions (power delay profiles, Doppler frequencies, antenna correlation). The considered simulation scenarios are completely specified by referring to sections and test numbers in TS 36.101. For example, in TS 36.101 Section 8.2.1.1.1, the tests for a single transmit antenna $N_T = 1$ and dual receive antenna $N_R = 2$ scenario are defined. By referring to test number one in this section, the AMC mode is defined as Quadrature Phase Shift Keying (QPSK) with a target coding rate of 1/3, Extended Vehicular A (EVEhA) channel model with a Doppler frequency of 5 Hz, and low antenna correlation. For our simulations presented here, we selected four test scenarios with a bandwidth of 10 MHz but different transmit modes (single antenna port transmission, OLSM, and TxD), different AMC schemes, and different channel models. Hybrid Automatic Repeat reQuest (HARQ) is supported with

²After all, the purpose of a simulation model is to abstract and thus simplify complex situations.

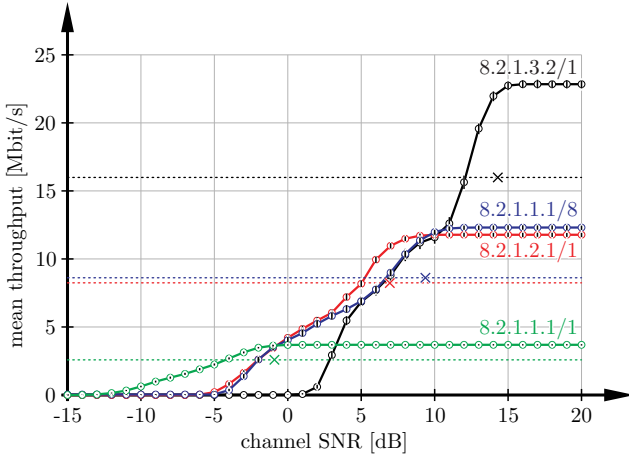


Fig. 8. Throughput simulations of the test scenarios in 3GPP TS 36.101 and comparison to the minimum performance requirements (marked with crosses). The small vertical bars within the circular markers indicate the 99% confidence intervals. Reproducible by running *Reproducibility_RAN_sims.m*.

at most three retransmissions. The most important parameters of the test scenarios are listed in Table I. The first scenario (8.2.1.1.1/1) refers to the test scenario described above. The OLSM scenario (8.2.1.3.2/1) utilizes a rank two transmission, that is, transmission of two spatial streams.

Simulation results for the considered scenarios are shown in Figure 8. The dashed horizontal lines correspond to 70% of the maximum throughput values for which TS 36.101 defines a channel Signal to Noise Ratio (SNR) requirement (shown as crosses in Figure 8). For all considered test scenarios, the link level simulator outperforms the minimum requirements by approximately 2-3 dB. The small vertical bars within the markers in Figure 8 are the 99% confidence intervals of the simulated mean throughput. Since the confidence intervals are much smaller than the distances between the individual throughput curves, we know that a repeated simulation with different seeds of the random number generators will lead to similar results and conclusions. Figure 8 can be reproduced by calling the script *Reproducibility_RAN_sims.m* included in the link level simulator.

B. Link and System Level Cross-Comparison

Next, we cross-compare the performance of the link and system level simulators. We consider a single-user single-cell scenario with different antenna configurations and transmit modes, as summarized in Table II.

In dependence of the channel conditions we adapt the AMC scheme, the transmission rank, and the precoding matrices. For this purpose, we utilize the UE feedback schemes originally presented in [16]. In order to create an equivalent simulation scenario on link and system level, we do not employ shadow fading. Whereas on link level the SNR is usually directly specified, on system level the SNR is a function of the user location in the cell. Without shadow fading, the user SNR on system level becomes a function of the distance between

TABLE II
TEST SCENARIOS FOR THE CROSS-COMPARISON OF THE LINK AND SYSTEM LEVEL SIMULATORS (SU CASE).

	SISO	TxD	OLSM	CLSM
channel	TU ³	TU	TU	TU
bandwidth	1.4 MHz	1.4 MHz	1.4 MHz	1.4 MHz
antenna conf.	1 × 1	2 × 2	2 × 2	4 × 2
CQI feedback	✓	✓	✓	✓
RI feedback	×	×	✓	✓
PMI feedback	×	×	×	✓
simulation time LL	3 200 s	9 500 s	19 500 s	14 200 s
simulation time SL	800 s	1 000 s	1 100 s	1 200 s
speed-up	4	9.5	17.7	11.8

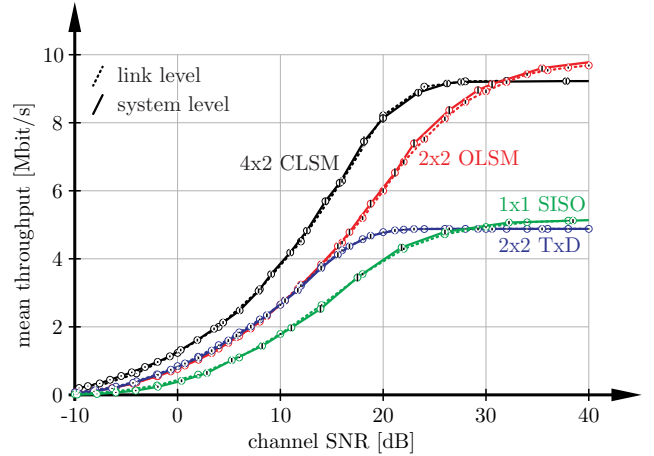


Fig. 9. Cross-comparison of throughput results obtained with the link level and the system level simulators. The small vertical bars within the circular markers indicate the 99% confidence intervals. Reproducible by running *Reproducibility_LLvsSL_batch.m*.

base-station and user. This can be utilized to indirectly select appropriate SNR values in the system level simulator. The results of the link and system level comparison are shown in Figure 9. For all considered simulation scenarios, we obtain an excellent match between the results of the two simulators, confirming the validity of our Link Error Prediction (LEP) model [54] on system level. Figure 9 can be reproduced by running the script *Reproducibility_LLvsSL_batch.m* provided in the system level simulator package. Further comparisons between link and system level simulator results are shown in Section V-B.

In Table II, we compare the simulation times of the link level simulator to those of the system level simulator. The simulations were conducted on one core of a 2.66 GHz Quad Core CPU. The table also states the simulation speed-up, defined as the ratio of the simulation times required with the link level and the system level simulator, respectively. The speed-up of the system level simulator for a Single-Input Single-Output (SISO) system equals four. This speed-up is rather small because equalization, demodulation, and decoding (tasks that are abstracted on system level) have low complexity in a SISO system. With increasing system complexity also the speed-

³TU: Typical Urban channel model [70].

up increases. We expected the largest speed-up in the CLSM scenario, because it utilizes the largest antenna configuration. However, we measured the largest speed-up of almost 18 in the OLSM simulation scenario. The reason is, that the precoder changes from one subcarrier to the next, while in the CLSM scenario, we assumed wideband feedback meaning that the same precoder is employed on all subcarriers [16].

The link level simulator supports the parallel computing capabilities of MATLAB. With these features it is possible to run several MATLAB instances in parallel on the multiple cores of a modern CPU. The simulation time of the link level simulator then decreases linearly with the number of CPU cores, while the system level simulator is currently not capable of parallel computing.

C. Further Validation Means

For a basic validation of the correctness of the results produced by the simulator, we checked the uncoded BER and throughput performance over frequency flat Rayleigh fading and AWGN channels, as the theoretical performance of these channels is known [71]. Furthermore, we cross-checked our results with results produced by other industry simulators, comparing to corresponding publications of the 3GPP RAN WG1, e.g., [31, 32]. Still, an open issue is to prove a correct functionality of each part of the simulator. Evaluation of the simulators has also been made possible for the whole research community, allowing everybody to modify the code to meet individual requirements and to check the code for correctness [72–74], as the simulator “changelog” reflects. The first versions of the simulators have been released in May 2009 (link level simulator) and in March 2010 (system level simulator), respectively. To facilitate the exchange of bugs and/or results often referred to as “crowdsourcing”, a forum⁴ is also provided. While the authors acknowledge this is not a perfect form of validation, neither is any other.

V. EXEMPLARY RESULTS

In this section, we show two exemplary simulation results obtained with the Vienna LTE simulators. Firstly, we present a link level throughput simulation in which we compare the throughput of the different MIMO schemes to theoretic bounds. Based on this simulation setup, researchers can investigate algorithms such as channel estimation, detection, or synchronization. Secondly, we compare the performance of different state-of-the-art schedulers in a single-cell multi-user environment. These schedulers serve as reference for researchers investigating advanced scheduling techniques.

⁴<http://www.nt.tuwien.ac.at/forum>

A. Link Level Throughput

Before presenting the link level throughput results of the different LTE MIMO schemes, we introduce theoretic bounds for the throughput. We identify three bounds, namely the mutual information, the channel capacity, and the so-called achievable mutual information. Depending on the type of channel state information available at the transmitter (only receive SNR, full, or quantized), an ideal transmission system is expected to attain one of these bounds.

1) *Mutual Information*: The mutual information is the theoretic bound for the data throughput if only the receive SNR but no further channel state information is available at the transmitter side [75]:

$$I = \sum_{k=1}^{N_{\text{tot}}} B_{\text{sub}} \log_2 \det \left(\mathbf{I}_{N_R} + \frac{1}{\sigma_n^2} \mathbf{H}_k \mathbf{H}_k^H \right) \quad (1)$$

Here, B_{sub} denotes the bandwidth occupied by a single data subcarrier, \mathbf{H}_k the $N_R \times N_T$ (= number of receive antennas \times number of transmit antennas) dimensional MIMO channel matrix of the k -th subcarrier, σ_n^2 the energy of noise and interference at the receiver, N_{tot} the total number of usable subcarriers, and \mathbf{I}_{N_R} an identity matrix of size equal to the number of receive antennas N_R . In Equation (1), we normalized the transmit power to one and the channel matrix according to $E\{\|\mathbf{H}_k\|_2^2\} = 1$. Therefore, Equation (1) does not show a dependence on the transmit power and the number N_T of transmit antennas.

The bandwidth B_{sub} of a subcarrier is calculated as

$$B_{\text{sub}} = \frac{N_s}{T_{\text{sub}} - T_{\text{cp}}}, \quad (2)$$

where N_s is the number of OFDM symbols in one subframe (usually equal to 14 when the normal cyclic prefix length is selected), T_{sub} the subframe duration (1 ms), and T_{cp} the time required for the transmission of all cyclic prefixes within one subframe. Note that we are calculating the mutual information for all *usable* subcarriers of the OFDM system, thereby taking into account the loss in spectral efficiency caused by the guard band carriers. If different transmission systems that apply different modulation formats are to be compared, however, a fair comparison would require calculating the mutual information over the entire system bandwidth instead of calculating it only over the usable bandwidth.

Current communication systems employ adaptive modulation and coding schemes to optimize the data throughput. For a specific receive SNR, assuming an optimum receiver, the modulation and coding scheme that maximizes the data throughput can be selected. Thus, if the transmitter knows the receive SNR, a throughput equal to the mutual information should be achieved.

2) *Channel Capacity*: For calculating the channel capacity of a frequency selective MIMO channel [71], consider the singular value decomposition of the channel matrix \mathbf{H}_k scaled by the standard deviation σ_n of the additive white Gaussian

TABLE III
PILOT SYMBOLS AND EFFICIENCY FACTOR F IN LTE.

transmit antennas N_T	reference symbols N_{ref}	efficiency factor F
1	4	88,88 %
2	8	84,44 %
4	12	80 %

677 noise impairment:

$$\frac{1}{\sigma_n} \mathbf{H}_k = \mathbf{U}_k \boldsymbol{\Sigma}_k \mathbf{V}_k^H \quad ; \text{ with} \quad (3)$$

$$\boldsymbol{\Sigma}_k = \text{diag} \left\{ \sqrt{\lambda_{k,m}} \right\} \quad m = 1 \dots \min(N_R, N_T)$$

678 The optimum, capacity-achieving, frequency-dependent pre-
679 coding at the transmitter is given by the unitary matrix \mathbf{V}_k . If
680 this precoding matrix is applied at the transmitter and also the
681 optimum receive filter \mathbf{U}_k^H is employed, the MIMO channel is
682 separated into $\min(N_R, N_T)$ (with N_R denoting the number of
683 receive antennas and N_T the number of transmit antennas)
684 independent SISO channels, each with a gain of $\sqrt{\lambda_{k,m}}$,
685 $m = 1 \dots \min(N_R, N_T)$, $k = 1 \dots N_{\text{tot}}$. The channel capacity
686 is obtained by optimally distributing the available transmit
687 power over these parallel SISO subchannels. The optimum
688 power distribution $P_{k,m}$ is the solution of the optimization
689 problem:

$$C = \max_{P_{k,m}} \frac{1}{N_{\text{tot}}} \sum_{m=1}^{\min(N_R, N_T)} \sum_{k=1}^{N_{\text{tot}}} \log_2 (1 + P_{k,m} \lambda_{k,m}) \quad (4)$$

$$\text{subject to} \quad \sum_{m=1}^{\min(N_R, N_T)} \sum_{k=1}^{N_{\text{tot}}} P_{k,m} = P_t.$$

690 Here, the second equation is a transmit power constraint that
691 ensures an average transmit power proportional to the number
692 of data subcarriers: $P_t = N_{\text{tot}}$. Note that due to the definition
693 of $\sqrt{\lambda_{k,m}}$ in Equation (3), the power distribution $P_{k,m}$ and
694 thus P_t remain dimensionless. We calculate the power coeffi-
695 cients maximizing Equation (4) by the water-filling algorithm
696 described in [71]. In order to achieve a throughput equal
697 to the channel capacity, the transmitter needs full channel
698 state information and has to apply the optimum precoder.
699 Furthermore, the receiver needs to apply the optimum receive
700 filter in order to separate the parallel SISO subchannels.

701 3) *Achievable Mutual Information*: Both mutual informa-
702 tion and channel capacity do not consider system design
703 losses caused for example by the transmission of cyclic prefix
704 or reference symbols, or the quantization of the transmitter
705 precoding. In order to obtain a tighter bound for the link level
706 throughput, we therefore consider these effects in the definition
707 of the so-called achievable mutual information. In the case
708 of open-loop transmission, in which space-time coding is
709 employed at the transmitter, we obtain for the achievable
710 mutual information

$$I_a^{(\text{OL})} = \sum_{k=1}^{N_{\text{tot}}} FB_{\text{sub}} \frac{1}{N_L} \log_2 \det \left(\mathbf{I}_{N_R N_L} + \frac{1}{\sigma_n^2} \tilde{\mathbf{H}}_k \tilde{\mathbf{H}}_k^H \right), \quad (5)$$

711 with N_L denoting the number of spatial transmission layers.
712 The $N_R N_L \times N_T$ dimensional matrix $\tilde{\mathbf{H}}_k$ is the effective chan-
713 nel matrix including the space-time coding [76]. The factor F

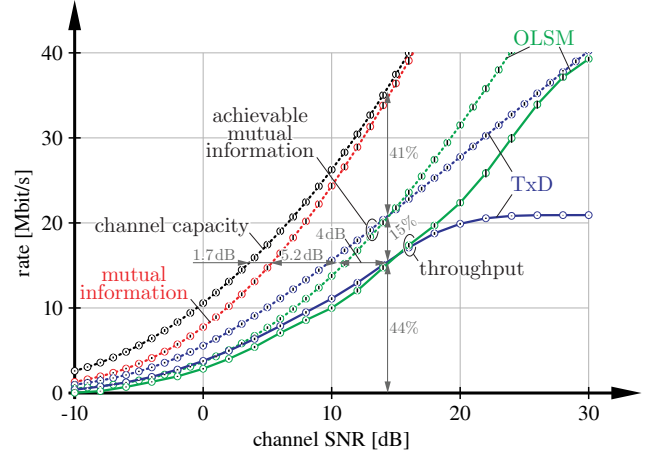


Fig. 10. Throughput of a 2×2 system with 5MHz bandwidth compared to the channel capacity, the mutual information, and the achievable mutual information. The small vertical bars within the circular markers indicate the 99% confidence intervals. Reproducible by running *Physical_Layer_batch.m*.

accounts for the inherent system losses due to the transmission
of the cyclic prefix and the reference symbols. In detail, the
factor F is calculated as

$$F = \underbrace{\frac{T_{\text{sub}} - T_{\text{cp}}}{T_{\text{sub}}}}_{\text{CP loss}} \cdot \underbrace{\frac{N_{\text{sc}} \cdot N_s / 2 - N_{\text{ref}}}{N_{\text{sc}} \cdot N_s / 2}}_{\text{reference symbols loss}}, \quad (6)$$

where N_{ref} is the number of reference symbols per resource
block, and $N_{\text{sc}} = 12$ is the number of subcarriers in each
RB. In LTE, the number of reference symbols depends on the
number of transmit antennas. Therefore, the efficiency factor
 F decreases with increasing number of transmit antennas (see
Table III).

In the case of closed-loop transmission, a channel adapted
precoding matrix \mathbf{W} is chosen from a set \mathcal{W} (defined in the
standard) and applied to the transmit signal. We calculate the
achievable mutual information for closed-loop transmission as:

$$I_a^{(\text{CL})} = \max_{\mathbf{W} \in \mathcal{W}} \sum_{k=1}^{N_{\text{tot}}} FB_{\text{sub}} \log_2 \det \left(\mathbf{I}_{N_R} + \frac{1}{\sigma_n^2} \mathbf{H}_k \mathbf{W} \mathbf{W}^H \mathbf{H}_k^H \right). \quad (7)$$

In Figure 10, the throughput of a 2×2 LTE system with
5MHz bandwidth, perfect channel knowledge, and a Soft
Sphere Decoder (SSD) receiver is shown and compared to
the previously presented theoretic bounds. The difference be-
tween channel capacity and mutual information is only small,
therefore, even knowledge of the full channel state information
at the transmitter does not considerably increase the potential
performance. In contrast, the difference between the mutual
information and the achievable mutual information is much
larger, resulting in a loss of 56% at an SNR of 15 dB. Most
(41%) of this loss is due to the restrictions implied by the
standard, as indicated by the achievable mutual information
curves in Figure 10. At a rate of 16 Mbit/s, the difference
between achievable mutual information and simulated throughput
is approximately 4 dB. These findings are similar to results

742 obtained when analyzing the performance of WiMAX and
 743 High-Speed Downlink Packet Access (HSDPA) in [77].

744 Figure 10 furthermore shows that for SNRs lower than
 745 14 dB, the TxD mode outperforms OLSM. Only at larger
 746 SNRs, above 20 dB, where the throughput of the TxD mode
 747 saturates, OLSM benefits from the second spatial stream and
 748 outperforms TxD.

749 Figure 10 can be reproduced by executing the script *Phys-*
 750 *ical_Layer_batch.m* provided in the Vienna LTE Link Level
 751 Simulator package.

752 B. LTE Scheduling

753 In this section, the performance of various multiuser LTE
 754 scheduling techniques is compared by means of link level
 755 and system level simulations. By appropriately selecting the
 756 simulation parameters in the link level, as well as the system
 757 level, we are able to show that the results obtained by the two
 758 simulators are equivalent.

759 In particular, we consider in the Vienna LTE System Level
 760 Simulator one sector of a single-cell SISO system with 20
 761 randomly positioned users. The user positions yield the large-
 762 scale path loss and shadow fading coefficients of all users
 763 and as a consequence, the average receive SNRs, which are
 764 distributed in a range of 2.7 dB to 36 dB. These average receive
 765 SNRs of the 20 users are set in the Vienna LTE Link Level
 766 Simulator to ensure the same propagation environment as on
 767 system level. Further simulation parameters of both simulators
 768 are summarized in Table IV.

769 The simulation results are averaged over 2 500 small-scale
 770 fading and noise realizations. In order to guarantee exactly
 771 the same channel realizations for all scheduler simulations on
 772 system level, the user positions, as well as the small- and large-
 773 scale fading realizations are loaded from pre-generated files.
 774 On link level, the seeds of the random number generators for
 775 fading and noise generation are set at the beginning of each
 776 simulation.

777 A performance comparison of different scheduling strategies
 778 is shown in Figures 11 and 12 in terms of total sector through-
 779 put and fairness (Jain’s fairness index [79]). The figures
 780 show that the results produced by the link and system level
 781 simulators are very similar for both throughput and fairness.

TABLE IV
 LINK AND SYSTEM LEVEL PARAMETERS FOR THE SCHEDULING
 SIMULATIONS.

Parameter	Value
system bandwidth	5 MHz
number of subcarriers	300
number of resource blocks	50
number of users	20
channel model	3GPP TU [78]
channel realizations	2 500
antenna configuration	1 transmit, 1 receive (1×1)
receiver	Zero Forcing (ZF)
schedulers	Best CQI (BCQI) maxmin proportional fair resource fair round robin

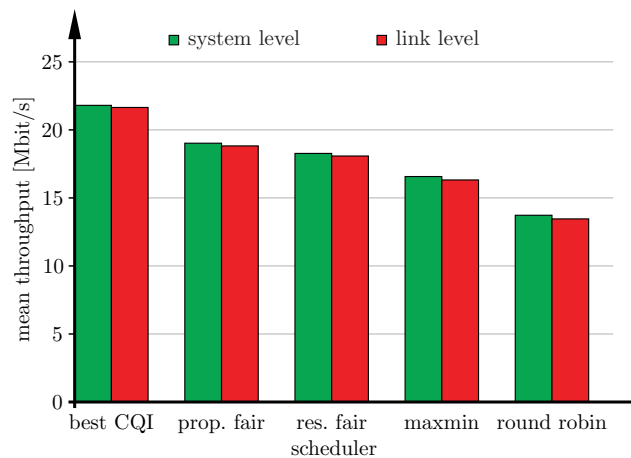


Fig. 11. Comparison of system throughput obtained with different scheduling strategies with link and system level simulations. Reproducible by running *Reproducibility_Schedulers_batch.m*.

The largest difference between the results of the two simulators is less than 2%, while the 99% confidence intervals (too small to be identified in the figures) of the simulated throughput are much smaller. Thus, we conclude that the system level simulator is properly calibrated; that is, the approximation and modeling of the link level does not result in large errors on system level.

The considered schedulers pursue different goals for resource allocation. The best CQI scheduler tries to maximize total throughput and completely ignores fairness by just assigning resources to the users with the best channel conditions. This is reflected in the simulation results in Figures 11 and 12, showing the highest system throughput and the lowest fairness for the best CQI scheduler. In contrast, the maxmin-scheduler assigns the resources in a way that equal throughput for all users is guaranteed, thereby maximizing Jain’s fairness index [79]. Round robin scheduling does not consider the user equipment feedback and cyclically assigns the same amount of resources to each user. Thus, ignoring the user equipment feedback results in the worst throughput performance of all schedulers consider here. The proportional fair scheduler emphasizes multiuser diversity by scheduling the user who has the best current channel realization relative to its own average. The resource fair scheduling strategy guarantees an equal amount of resources for all users while trying to maximize the total throughput. In the simulations, the proportional fair strategy outperforms resource fair in terms of throughput as well as fairness thereby resulting in a good trade-off between throughput and fairness. Further details about the implemented schedulers, as well as more simulation results, can be found in [24].

The presented simulation results can be reproduced by calling the script *Reproducibility_Schedulers_batch.m* that can be found in the directory “paper scripts” of the link level and the system level simulator, respectively. More examples of the Vienna LTE simulators also in the context of LTE-Advanced are presented in [80].

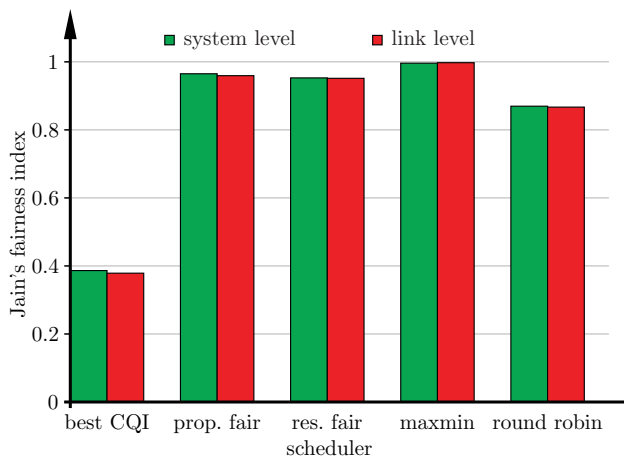


Fig. 12. Comparison of fairness obtained with different scheduling strategies with link and system level simulations. Reproducible by running *Reproducibility_Schedulers_batch.m*.

VI. CONCLUSIONS

In this paper, we presented the Vienna LTE Simulators, consisting of a link level and a system level simulator. Both simulators are available under a non-commercial open source academic-use license and thereby enable researchers to implement and test algorithms in the context of LTE. The open source availability of the simulators facilitates researchers to reproduce published results in the context of LTE, and thus supports the comparison of novel algorithms with previous state-of-the-art. So far (March 2011), the simulators have been downloaded more than 13 000 times from all over the world.

ACKNOWLEDGMENTS

This work has been funded by the Christian Doppler Laboratory for Wireless Technologies for Sustainable Mobility, KATHREIN-Werke KG, and A1 Telekom Austria AG. The financial support by the Federal Ministry of Economy, Family and Youth and the National Foundation for Research, Technology and Development is gratefully acknowledged. The authors would like to thank Christoph F. Mecklenbräuer for his valuable comments and fruitful discussions.

REFERENCES

[1] [Online]. Available: <http://www.nt.tuwien.ac.at/ltesimulator/>

[2] M. Barni and F. Perez-Gonzalez, "Pushing science into signal processing," *IEEE Signal Process. Mag.*, vol. 22, no. 4, pp. 120–119, July 2005, doi: 10.1109/MSP.2005.1458324.

[3] P. Vandewalle, J. Kovačević, and M. Vetterli, "Reproducible research in signal processing," *IEEE Signal Process. Mag.*, vol. 26, no. 3, pp. 37–47, May 2009, doi: 10.1109/MSP.2009.932122.

[4] M. Dohler, R. Heath Jr., A. Lozano, C. B. Papadias, and R. A. Valenzuela, "Is the PHY layer dead?" *IEEE Communications Magazine*, no. 4, pp. 159–165, Apr. 2011.

[5] J. B. Buckheit and D. L. Donoho, "Wavelab and reproducible research," Dept. of Statistics, Stanford Univ., Tech. Rep. 474, Tech. Rep., 1995. [Online]. Available: <http://www-stat.stanford.edu/~donoho/Reports/1995/wavelab.pdf>

[6] P. Vandewalle, S. Süsstrunk, and M. Vetterli, "A frequency domain approach to registration of aliased images with application to super-resolution," *EURASIP Journal on Applied Signal Processing*, vol. 2006, Article ID 71459, 2006, doi: 10.1155/ASP/2006/71459.

[7] C. Mehlführer, S. Caban, and M. Rupp, "Experimental evaluation of adaptive modulation and coding in MIMO WiMAX with limited feedback," *EURASIP Journal on Advances in Signal Processing, Special Issue on MIMO Systems with Limited Feedback*, vol. 2008, Article ID 837102, 2008, doi: 10.1155/2008/837102.

[8] M. Šimko, D. Wu, C. Mehlführer, J. Eilert, and D. Liu, "Implementation Aspects of Channel Estimation for 3GPP LTE Terminals," in *Proc. European Wireless (EW 2011)*, Vienna, Austria, Apr. 2011.

[9] R. Dallinger, H. Ruotsalainen, R. Wichman, and M. Rupp, "Adaptive pre-distortion techniques based on orthogonal polynomials," in *Conference Record of the 44th Asilomar Conference on Signals, Systems and Computers*, Pacific Grove (CA), USA, Nov. 2010.

[10] Technical Specification Group RAN, "E-UTRA; LTE physical layer – general description," 3GPP, Tech. Rep. TS 36.201 Version 8.3.0, March 2009.

[11] International Telecommunication Union ITU, "Requirements related to technical performance for IMT-advanced radio interface(s), ITU-R M.2134," online, ITU-R M.2134, <http://www.itu.int/pub/R-REP-M.2134-2008/en>.

[12] Technical Specification Group RAN, "E-UTRA; further advancements for E-UTRA physical layer aspects," 3GPP, Tech. Rep. TS 36.814, Mar. 2010.

[13] C. Williams, S. McLaughlin, and M. A. Beach, "Exploiting multiple antennas for synchronization," *IEEE Trans. Veh. Technol.*, vol. 58, no. 2, pp. 773–787, Feb. 2009, doi: 10.1109/TVT.2008.925309.

[14] Q. Wang, S. Caban, C. Mehlführer, and M. Rupp, "Measurement based throughput evaluation of residual frequency offset compensation in WiMAX," in *Proc. 51st International Symposium ELMAR-2009*, pp. 233–236, Zadar, Croatia, Sept. 2009.

[15] N. Kolehmainen, J. Puttonen, P. Kela, T. Ristaniemi, T. Henttonen, and M. Moisiö, "Channel quality indication reporting schemes for UTRAN long term evolution downlink," in *Proc. IEEE Vehicular Technology Conference Spring (VTC)*, pp. 2522–2526, May 2008.

[16] S. Schwarz, C. Mehlführer, and M. Rupp, "Calculation of the spatial preprocessing and link adaption feedback for 3GPP UMTS/LTE," in *Proc. IEEE Wireless Advanced*, doi: 10.1109/WIAD.2010.5544947, London, UK, June 2010.

[17] L. Boher, R. Legouable, and R. Rabineau, "Performance analysis of iterative receiver in 3GPP/LTE DL MIMO OFDMA system," in *Proc. IEEE 10th International Symposium on Spread Spectrum Techniques and Applications (ISSSTA)*, pp. 103–108, doi: 10.1109/ISSSTA.2008.26, Aug. 2008.

[18] J. C. Ikuno, M. Wrulich, and M. Rupp, "Performance and modeling of LTE H-ARQ," in *Proc. International ITG Workshop on Smart Antennas (WSA 2009)*, Berlin, Germany, Feb. 2009.

[19] M. Wrulich and M. Rupp, "Computationally efficient MIMO HSDPA system-level modeling," *EURASIP Journal on Wireless Communications and Networking*, vol. 2009, Article ID 382501, 2009, doi: 10.1155/2009/382501.

[20] T. M. Cover, "Comments on broadcast channels," *IEEE Trans. Inf. Theory*, vol. 44, no. 6, pp. 2524–2530, Oct. 1998, doi: 10.1109/18.720547.

[21] H. Weingarten, Y. Steinberg, and S. Shamai, "The capacity region of the gaussian multiple-input multiple-output broadcast channel," *IEEE Trans. Inf. Theory*, vol. 52, no. 9, pp. 3936–3964, Sept. 2006, doi: 10.1109/TIT.2006.880064.

[22] U. Niesen, P. Gupta, and D. Shah, "The balanced unicast and multicast capacity regions of large wireless networks," *IEEE Trans. Inf. Theory*, vol. 56, no. 5, pp. 2249–2271, May 2010, doi: 10.1109/TIT.2010.2043979.

[23] D. Skoutas, D. Komninos, D. Vouyioukas, and A. Rouskas, "Enhanced dedicated channel scheduling optimization in WCDMA," in *Proc. 14th European Wireless Conference (EW)*, doi: 10.1109/EW.2008.4623867, June 2008.

[24] S. Schwarz, C. Mehlführer, and M. Rupp, "Low complexity approximate maximum throughput scheduling for LTE," in *Conference Record of the 44th Asilomar Conference on Signals, Systems and Computers*, Pacific Grove, CA, USA, Nov. 2010.

[25] K. Peppas, T. Al-Gizawi, F. Lazarakis, D. Axiotis, A. Moussa, and A. Alexiou, "System level evaluation of reconfigurable MIMO techniques enhancements for HSDPA," in *Proc. IEEE Global Telecommunications Conference (GLOBECOM)*, vol. 5, pp. 2869–2873, doi: 10.1109/GLOCOM.2004.1378879, 2004.

[26] P. Konis, D. Kalamani, and G. Tsoulos, "Capacity of WCDMA multicellular networks under different radio resource management strategies," in *Proc. 3rd International Symposium on Wireless Pervasive Computing (ISWPC)*, pp. 60–64, doi: 10.1109/ISWPC.2008.4556166, 2008.

[27] M. Castañeda, M. Ivrlac, J. Nossek, I. Viering, and A. Klein, "On

- downlink intercell interference in a cellular system,” in *Proc. IEEE 18th International Symposium on Personal, Indoor and Mobile Radio Communications (PIMRC)*, pp. 1–5, doi: 10.1109/PIMRC.2007.4394052, 2007.
- [28] T. Nihtila and V. Haikola, “HSDPA MIMO system performance in macro cell network,” in *Proc. IEEE Sarnoff Symposium*, doi: 10.1109/SARNOF.2008.4520092, 2008.
- [29] K. I. Pedersen, T. F. Lootsma, M. Stottrup, F. Frederiksen, T. Kolding, and P. E. Mogensen, “Network performance of mixed traffic on high speed downlink packet access and dedicated channels in WCDMA,” in *Proc. IEEE 60th Vehicular Technology Conference (VTC)*, vol. 6, pp. 4496–4500, doi: 10.1109/VETEFCF.2004.1404930, 2004.
- [30] S. A. Jafar and M. J. Fakhreddin, “Degrees of freedom for the MIMO interference channel,” *IEEE Trans. Inf. Theory*, vol. 53, no. 7, pp. 2637–2642, July 2007, doi: 10.1109/TIT.2007.899557.
- [31] Nortel, “Performance evaluation of CL MIMO under different UE speed,” 3rd Generation Partnership Project (3GPP), Tech. Rep. R1-080384, Jan. 2008.
- [32] Nokia & Nokia-Siemens-Networks, “LTE performance benchmarking,” 3rd Generation Partnership Project (3GPP), Tech. Rep. R1-071960, Apr. 2007.
- [33] steepest ascent. (2009) 3GPP LTE toolbox and blockset.
- [34] mimoOn. (2009) mi!mobile.
- [35] Aricent. (2009) LTE layer 1 – LTE baseband / PHY library.
- [36] J. J. Sánchez, G. Gómez, D. Morales-Jiménez, and J. T. Entrambasaguas, “Performance evaluation of OFDMA wireless systems using WM-SIM platform,” in *Proc. ACM 4th International Workshop on Mobility Management and Wireless Access (MobiWac)*, pp. 131–134, doi: 10.1145/1164783.1164808, 2006.
- [37] C. Mehlführer, M. Wrulich, J. C. Ikuno, D. Bosanska, and M. Rupp, “Simulating the long term evolution physical layer,” in *Proc. 17th European Signal Processing Conference (EUSIPCO 2009)*, pp. 1471–1478, Glasgow, Scotland, UK, Aug. 2009.
- [38] J. C. Ikuno, M. Wrulich, and M. Rupp, “System level simulation of LTE networks,” in *Proc. 2010 IEEE 71st Vehicular Technology Conference (VTC2010-Spring)*, doi: 10.1109/VETECS.2010.5494007, Taipei, Taiwan, May 2010.
- [39] Technical Specification Group RAN, “E-UTRA; physical channels and modulation,” 3GPP, Tech. Rep. TS 36.211 Version 8.7.0, May 2009.
- [40] Technical Specification Group RAN, “E-UTRA; multiplexing and channel coding,” 3GPP, Tech. Rep. TS 36.212, March 2009.
- [41] Technical Specification Group RAN, “E-UTRA; physical layer procedures,” 3GPP, Tech. Rep. TS 36.213, March 2009.
- [42] X. Wang, G. Giannakis, and A. Marques, “A unified approach to QoS-guaranteed scheduling for channel-adaptive wireless networks,” *Proceedings of the IEEE*, vol. 95, no. 12, pp. 2410–2431, Dec. 2007, doi: 10.1109/JPROC.2007.907120.
- [43] C. L. Raymond Kwan and J. Zhang, “Multiuser scheduling on the downlink of an LTE cellular system,” *Research Letters in Communications*, vol. 2008, Article ID 323048, 2008, doi: 10.1155/2008/323048.
- [44] S. Schwarz, C. Mehlführer, and M. Rupp, “Throughput maximizing multiuser scheduling with adjustable fairness,” in *Proc. IEEE International Conference on Communications (ICC 2011)*, Kyoto, Japan, May 2011.
- [45] Members of ITU, “Recommendation ITU-R M.1225: Guidelines for evaluation of radio transmission technologies for IMT-2000,” International Telecommunication Union (ITU), Tech. Rep., 1997.
- [46] L. Hentilä, P. Kyösti, M. Käske, M. Narandzic, and M. Alatossava, “MATLAB implementation of the WINNER phase ii channel model ver1.1,” Dec. 2007. [Online]. Available: http://www.ist-winner.org/phase_2_model.html
- [47] M. Šimko, C. Mehlführer, M. Wrulich, and M. Rupp, “Doubly dispersive channel estimation with scalable complexity,” in *Proc. International ITG Workshop on Smart Antennas (WSA 2010)*, pp. 251–256, doi: 10.1109/WSA.2010.5456443, Bremen, Germany, Feb. 2010.
- [48] Q. Wang, C. Mehlführer, and M. Rupp, “Carrier frequency synchronization in the downlink of 3GPP LTE,” in *Proc. 21st Annual IEEE International Symposium on Personal, Indoor and Mobile Radio Communications (PIMRC 2010)*, Istanbul, Turkey, Sept. 2010.
- [49] M. Šimko, C. Mehlführer, T. Zemen, and M. Rupp, “Inter carrier interference estimation in MIMO OFDM systems with arbitrary pilot structure,” in *Proc. 73rd IEEE Vehicular Technology Conference (VTC2011-Spring)*, Budapest, Hungary, May 2011.
- [50] I. Solutions, “Iterative Solutions Coded Modulation Library (ISCML).” [Online]. Available: <http://www.iterativesolutions.com/>
- [51] T. Pircher, “pycrc CRC calculator and C source code generator.” [Online]. Available: <http://www.tty1.net/pycrc/>
- [52] Q. Wang, C. Mehlführer, and M. Rupp, “SNR optimized residual frequency offset compensation for WiMAX with throughput evaluation,” in *Proc. 17th European Signal Processing Conference (EUSIPCO 2009)*, Glasgow, Scotland, UK, Aug. 2009.
- [53] L. Boher, R. Legouable, and R. Rabineau, “Performance analysis of iterative receiver in 3GPP/LTE DL MIMO OFDMA system,” in *Proc. IEEE 10th International Symposium on Spread Spectrum Techniques and Applications 2008 (ISSSTA 2008)*, pp. 103–108, doi: 10.1109/ISSSTA.2008.26, Aug. 2008.
- [54] J. C. Ikuno, C. Mehlführer, and M. Rupp, “A novel link error prediction model for OFDM systems with HARQ,” in *Proc. IEEE International Conference on Communications (ICC 2011)*, Kyoto, Japan, May 2011.
- [55] M. Wrulich, S. Eder, I. Viering, and M. Rupp, “Efficient link-to-system level model for MIMO HSDPA,” in *Proc. of the 4th IEEE Broadband Wireless Access Workshop*, doi: 10.1109/GLOCOMW.2008.ECP.83, New Orleans, LA, USA, Dec. 2008.
- [56] C. Mehlführer, M. Wrulich, and M. Rupp, “Intra-cell interference aware equalization for TxAA HSDPA,” in *Proc. 3rd IEEE International Symposium on Wireless Pervasive Computing (ISWPC 2008)*, pp. 406–409, doi: 10.1109/ISWPC.2008.4556239, Santorini, Greece, May 2008.
- [57] A. Ibing and V. Jungnickel, “Joint transmission and detection in hexagonal grid for 3GPP LTE,” in *Proc. International Conference on Information Networking 2008 (ICOIN 2008)*, doi: 10.1109/ICOIN.2008.4472825, Jan. 2008.
- [58] V. Cadambe and S. Jafar, “Interference alignment and degrees of freedom of the K-user interference channel,” *IEEE Trans. Inf. Theory*, vol. 54, no. 8, pp. 3425–3441, Apr. 2008, doi: 10.1109/TIT.2008.926344.
- [59] R. Treshch and M. Guillaud, “Cellular interference alignment with imperfect channel knowledge,” in *IEEE International Conference on Communications Workshops 2009 (ICC Workshops 2009)*, doi: 10.1109/ICCW.2009.5208018, June 2009.
- [60] P. Wu and N. Jindal, “Performance of hybrid-ARQ in block-fading channels: A fixed outage probability analysis,” *IEEE Transactions on Communications*, vol. 58, no. 4, pp. 1129–1141, Apr. 2010, doi: 10.1109/TCOMM.2010.04.080622.
- [61] Y. Blankenship, P. Sartori, B. Classon, V. Desai, and K. Baum, “Link error prediction methods for multicarrier systems,” in *Proc. IEEE 60th Vehicular Technology Conference (VTC2004-Fall)*, vol. 6, pp. 4175–4179, doi: 10.1109/VETEFCF.2004.1404865, Sept. 2004.
- [62] Technical Specification Group RAN, “E-UTRA; LTE RF system scenarios,” 3GPP, Tech. Rep. TS 36.942, 2008-2009.
- [63] T. Zemen and C. Mecklenbräuker, “Time-variant channel estimation using discrete prolate spheroidal sequences,” *IEEE Trans. Signal Process.*, vol. 53, no. 9, pp. 3597–3607, Sept. 2005, doi: 10.1109/TSP.2005.853104.
- [64] J. Kim, A. Ashikhmin, A. van Wijngaarden, E. Soljanin, and N. Gopalakrishnan, “On efficient link error prediction based on convex metrics,” in *Proc. IEEE 60th Vehicular Technology Conference (VTC2004-Fall)*, vol. 6, pp. 4190–4194, doi: 10.1109/VETEFCF.2004.1404869, Sept. 2004.
- [65] S. Tsai and A. Soong, “Effective-SNR mapping for modeling frame error rates in multiple-state channels,” 3GPP2, Tech. Rep. 3GPP2-C30-20030429-010, Apr. 2003.
- [66] L. Wan, S. Tsai, and M. Almgren, “A fading-insensitive performance metric for a unified link quality model,” in *Proc. IEEE Wireless Communications and Networking Conference (WCNC2006)*, vol. 4, pp. 2110–2114, doi: 10.1109/WCNC.2006.1696622, Apr. 2006.
- [67] Technical Specification Group RAN, “Physical layer aspects for E-UTRA,” 3GPP, Tech. Rep. TS 25.814, 2006.
- [68] H. Claussen, “Efficient modelling of channel maps with correlated shadow fading in mobile radio systems,” in *Proc. IEEE 16th International Symposium on Personal, Indoor and Mobile Radio Communications (PIMRC2005)*, vol. 1, pp. 512–516, doi: 10.1109/PIMRC.2005.1651489, Sept. 2005.
- [69] Technical Specification Group RAN, “Evolved universal terrestrial radio access (E-UTRA); user equipment (UE) radio transmission and reception,” 3GPP, Tech. Rep. TS 36.101 Version 8.5.1, Mar. 2009.
- [70] 3GPP, “Technical Specification Group Radio Access Networks; Deployment aspects (Release 8),” Dec. 2008, [Online]. Available: <http://www.3gpp.org/ftp/Specs/html-info/25943.htm>.
- [71] A. Paulraj, R. Nabar, and D. Gore, *Introduction to Space-Time Wireless Communications*, 1st ed. Cambridge Univ. Press, 2003.
- [72] Y. Feng, A. Krewski, and W. L. Schroeder, “Simulation based comparison of metrics and measurement methodologies for OTA test of MIMO terminals,” in *Proc. of the Fourth European Conference on*

- 1089 *Antennas and Propagation (EuCAP 2010)*, Apr. 2010.
- 1090 [73] V. H. Muntean, M. Oteşteanu, and G.-M. Muntean, "QoS parameters
1091 mapping for the e-learning traffic mix in LTE networks," in
1092 *Proc. International Joint Conference on Computational Cybernetics
1093 and Technical Informatics (ICCC-CONTI 2010)*, pp. 299–304, doi:
1094 10.1109/ICCCYB.2010.5491266, May 2010.
- 1095 [74] D. Wu, J. Eilert, R. Asghar, and D. Liu, "VLSI implementation of a
1096 fixed-complexity soft-output MIMO detector for high-speed wireless,"
1097 *EURASIP Journal on Wireless Communications and Networking*, vol.
1098 2010, Article ID 893184, 2010, doi: 10.1155/2010/893184.
- 1099 [75] C. Mehlführer, S. Caban, and M. Rupp, "Measurement-
1100 based performance evaluation of MIMO HSDPA," *IEEE
1101 Transactions on Vehicular Technology*, accepted for publication,
1102 doi: 10.1109/TVT.2010.2066996.
- 1103 [76] B. Badic, M. Rupp, and H. Weinrichter, "Adaptive channel-matched
1104 extended alamouti space-time code exploiting partial feedback," *ETRI
1105 Journal*, vol. vol. 26, no. no. 5, pp. 443–451, 2004.
- 1106 [77] M. Rupp, C. Mehlführer, and S. Caban, "On achieving the Shannon
1107 bound in cellular systems," in *Proc. 20th International Conference
1108 Radioelektronika 2010*," doi: 10.1109/RADIOELEK.2010.5478551,
1109 Brno, Czech Republik, Apr. 2010.
- 1110 [78] Technical Specification Group Radio Access Network, "Deployment
1111 aspects (Release 8)," 3GPP, Tech. Rep. TS 25.943 Version 8.0, Dec.
1112 2008.
- 1113 [79] R. Jain, D. Chiu, and W. Hawe, "A Quantitative Measure of Fairness and
1114 Discrimination for Resource Allocation in Shared Computer Systems,"
1115 DEC, Tech. Rep. TR-301, September 1984.
- 1116 [80] S. Caban, C. Mehlführer, M. Rupp, and M. Wrulich, *Evaluation of
1117 HSDPA and LTE, From Testbed Measurements to System Level Per-
1118 formance*. Wiley, 2011.